Organometallic Chemistry

Deutsche Ausgabe: DOI: 10.1002/ange.201607648
Internationale Ausgabe: DOI: 10.1002/anie.201607648

Redox Non-Innocent Behavior of a Terminal Iridium Hydrazido(2−) Triple Bond

*Adam J. Pearce, Alyssa A. Cassabaum, Grace E. Gast, Renee R. Frontiera, and Ian A. Tonks**

Abstract: *The synthesis of the first terminal Group 9 hydrazido(2-) complex, Cp*IrN(TMP) (**6**) (TMP = 2,2,6,6-tetramethylpiperidine) is reported. Electronic structure and X-ray diffraction analysis indicate that this complex contains an Ir−N triple bond, similar to Bergman's seminal Cp*Ir(N^{t}Bu) imido complex. However, in sharp contrast to Bergman's imido, **6** displays remarkable redox non-innocent reactivity owing to the presence of the N_β lone pair. Treatment of **6** with MeI results in electron transfer from N_β to Ir prior to oxidative addition of MeI to the iridium center. This behavior opens the possibility of carrying out facile oxidative reactions at a formally Ir^{III} metal center through a hydrazido(2−)/isodiazene valence tautomerization.*

Late transition metal–ligand multiple bonding plays a significant role in many organic transformations, such as C−H bond functionalization[1–3] and group transfer reactions.[4] Consequently, the field has experienced substantial growth in the past 25 years: several imido and oxo complexes of the late transition metals (Groups 8–10) have been synthesized,[5–12] but examples of heteroatom-functionalized multiply bound ligands, such as terminal hydrazido(2−) and alkoxyimidos, are extremely limited.[13] Such terminal moieties are attractive synthetic targets because they are important intermediates along N_2 reduction cycles and in other catalytic reactions, in which they can serve as built-in oxidants through cleavage of the *N*-heteroatom bond.[14–16] Furthermore, terminal hydrazidos have the potential to access redox non-innocent[17] manifolds through a contribution from the β-N lone pair (hydrazido(2−)/1,1-isodiazene resonance),[18] which may allow for redox reactions that would be otherwise inaccessible without such metal–ligand cooperativity.

Several early and mid-transition metal hydrazido(2−) complexes[19–25] have been synthesized through salt metathesis, protonolysis, or activation of N_2.[13,26] However, there are no isolated examples of terminal late transition metal (Groups 9 and 10) hydrazido(2−) complexes, and only a single example has been proposed as an intermediate in catalysis. In this reported example, Lu implicates a Co hydrazido(2−) as an intermediate in N_2 functionalization.[27] The closest isolated analogue to a Group 9 hydrazido(2−) was reported by Hartwig, who isolated the isomeric 1,1-isodiazene complex (PCP)IrNNC$_5$H$_{10}$.[28] In this case, the neutral 1,1-isodiazene electronic structure must dominate because the hydrazido(2−) form would violate the oxo wall of the square-planar ligand field. This is borne out in the structural parameters and reactivity of the complex, which has a short N−N bond (1.244(16) Å), long Ir−N bond (2.008(11) Å), and reactivity that mirrors that of free aminonitrenes. As a result of the dearth of Group 9 examples, we sought to synthesize iridium hydrazido(2−) complexes and investigate their electronic structure and reactivity. Herein, we report the first example of a terminal hydrazido(2−) complex of a late transition metal and report preliminary reactivity that demonstrates the unique redox non-innocent behavior of the terminal moiety, as well as the synthesis and differential reactivity of related hydrazido dimers.

The synthesis for Cp*-based iridium hydrazidos is reported in Scheme 1. Following Glueck and Bergman's synthesis of Cp*IrN^{t}Bu,[29] initial attempts to synthesize a monomeric hydrazido using lithium 1,1-diphenylhydrazide or lithium 1,1-dimethylhydrazide resulted in dimeric products

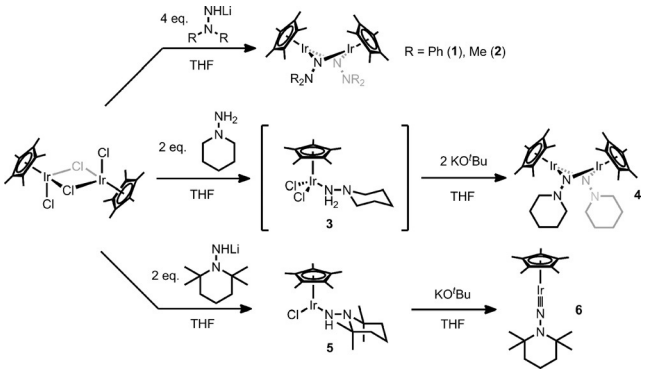

Scheme 1. Synthesis of compounds **1**–**6**.

[Cp*Ir(μ_2-N$_2$Ph$_2$)]$_2$ (**1**) and [Cp*Ir(μ_2-N$_2$Me$_2$)]$_2$ (**2**). Similarly, treatment of [Cp*IrCl$_2$]$_2$ with *N*-aminopiperidine followed by a double dehydrohalogenation of the resulting Ir hydrazine adduct **3** with two equivalents of KO^{t}Bu affords a third dimeric product [Cp*Ir (μ_2-NNC$_5$H$_{10}$)]$_2$ (**4**). Dimerization of analogous imido complexes with small *N*-substituents is well established.[30,31] To increase the steric profile of the β-N substituent, reactions were attempted with 1-amino-2,2,6,6-tetramethylpiperidine (NH$_2$TMP). Treatment of [Cp*IrCl$_2$]$_2$ with two equivalents of LiNHTMP yielded a deep red solution of Cp*IrCl(NHTMP) (**5**). Interestingly, unlike the other hydrazides, **5** was unable to be dehydrohalogenated by addition of further equivalents of LiNHTMP under standard

[*] A. J. Pearce, A. A. Cassabaum, G. E. Gast, Prof. Dr. R. R. Frontiera, Prof. Dr. I. A. Tonks
Department of Chemistry, University of Minnesota—Twin Cities
207 Pleasant St SE, Minneapolis, MN 55455 (USA)
E-mail: itonks@umn.edu

Supporting information for this article can be found under: http://dx.doi.org/10.1002/anie.201607648.

reaction conditions. However, the addition of KO^{t}Bu resulted in the formation of the monomeric terminal hydrazido(2−) Cp*IrNTMP (**6**) as a gold-colored solid in high yield.

The crystal structures of compounds **1**, **2**, **4**, and **6** are shown in Figure 1. The structure of **6** contains two independent molecules within the asymmetric unit. The bonding metrics confirm **6** as a terminally bound hydrazido(2−) that contains an Ir–N triple bond. The Ir–N bond distances

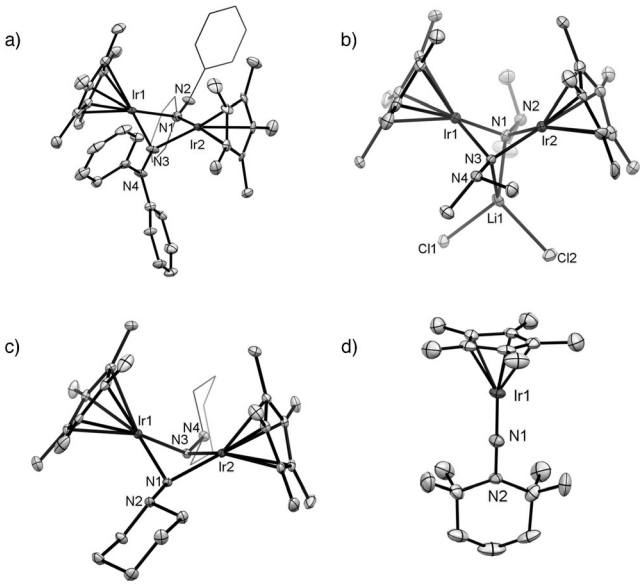

Figure 1. ORTEP of a) [Cp*Ir(N_2Ph_2)]$_2$ (**1**)), b) [Cp*Ir(N_2Me_2)]$_2$·LiCl (**2**), c) [Cp*Ir(NPip)]$_2$ (**4**), and d) Cp*IrNTMP (**6**). Thermal ellipsoids are drawn at 50% probability. Hydrogen atoms, solvent molecules, half a tetrameric unit of **2**, and a crystallographically independent molecule of **6** have been omitted for clarity. For complete crystallographic data, see Ref. [35].

(1.714(3) and 1.721(3) Å) are similar to the Ir–N distance observed in Bergman's Ir–N triple-bonded Cp*IrN^{t}Bu complex (1.712(7) Å). The N_α–N_β distances (1.340(5) Å and 1.342(4) Å) are significantly shorter than in the dimeric structures **1**, **2**, and **4** (1.384, 1.43, and 1.413 Å, respectively; see Table 1). This is consistent with strong π-donation to Ir from N_α in **6**, which reduces N_α–N_β lone pair repulsion. A significant difference in the Ir–N_α–N_β bond angles exists between the two independent molecules of **6** (178.3(3)° and 166.8(3)°); however, Parkin and Bercaw have argued that steric/crystal packing factors contribute more to the crystalographic bond angles in metal–N multiple bonds than the

Table 1: Selected bond distances (Å) and angles [°] for compounds **1**, **2**, **4**, and **6**.

Bond	**1**[a]	**2**[a]	**4**[a]	**6**[b]
Ir–Nα	1.982	1.99	1.983	1.718
Nα–Nβ	1.384	1.43	1.413	1.341
Ir–$Cp_{centroid}$	1.836	1.837	1.846	1.842
Ir–Nα–Nβ	129.8	126.1	127.1	172.3

[a] Average values for both Ir centers. [b] Average values for two crystallographically independent monomers.

hybridization at N.[32] In contrast, the bonding metrics of **6** are significantly different from Hartwig's 1,1-isodiazene complex (PCP)IrNNC$_5$H$_{10}$, which contains a long Ir–N distance, 2.008(11) Å; a short N_α–N_β distance, 1.244(16) Å; and an Ir–N_α–N_β bond angle of 135.1(12)°.[28]

A qualitative MO description of the relevant π orbitals of **6** is shown in Figure 2. In contrast to normal metal imidos, the N_β lone pair mixes with one of the Ir–N π-bonds, which results in a bonding and antibonding combination.[18] This removes the degeneracy of the Ir–N π-bonds and yields a HOMO

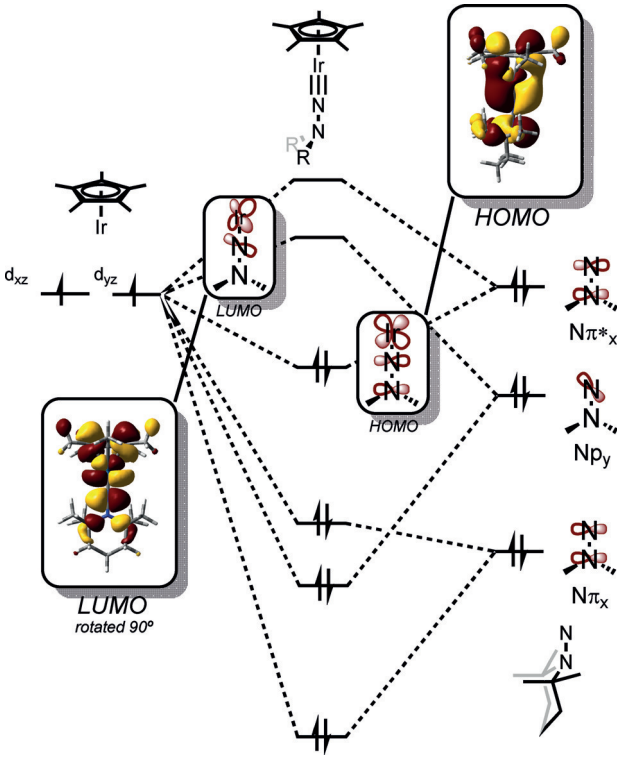

Figure 2. Qualitative MO diagram of compound **6** showing relevant π-bonding and antibonding combinations of Ir d-orbitals and diazene π-orbitals, as well as the DFT-calculated HOMO and LUMO.

comprised of Ir–N_α π-bonding and N_α–N_β π-antibonding interactions. This antibonding contribution raises the energy of the HOMO relative to the LUMO, which is the Ir–N_α π-antibonding orbital that is out of plane with the β-nitrogen lone pair. DFT calculations (M06-L/MWB60 on Ir; 6-31G(d) on C and H; 6-311 + G(2df,p) on N) provide a HOMO–LUMO energy gap of 409 nm, which is in good agreement with the experimental UV/Vis spectrum of **6**, which shows an absorbance shoulder at 400 nm. The resonance Raman spectrum (514.5 nm excitation) shown in Figure 3 also agrees with the DFT calculations, enhancing N–N, Ir–N, and C–C stretching frequencies predicted for the HOMO, and the N–N and Ir–N frequencies are in excellent agreement with related third row metal hydrazidos.[18]

With terminal and bridged Ir hydrazides in hand, we were interested in exploring the differential reactivity of the series in comparison to Bergman's terminal Ir imido. A summary of [Cp*IrNR]$_x$ reactivity with CO is shown in Scheme 2.

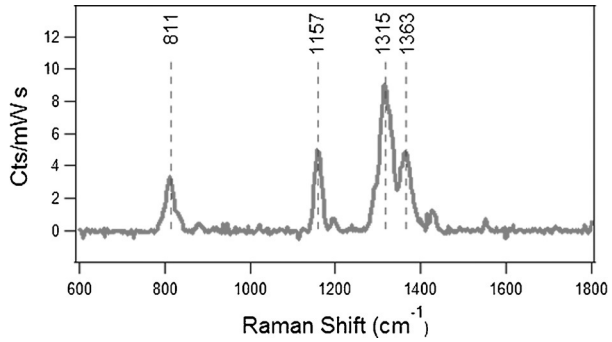

Figure 3. Resonance Raman spectrum of Cp*IrNTMP (**6**), showing features attributed to N–N (811, 1315 cm^{-1}), Ir–N (1157 cm^{-1}), and C–C (1365 cm^{-1}) bond stretching frequencies.

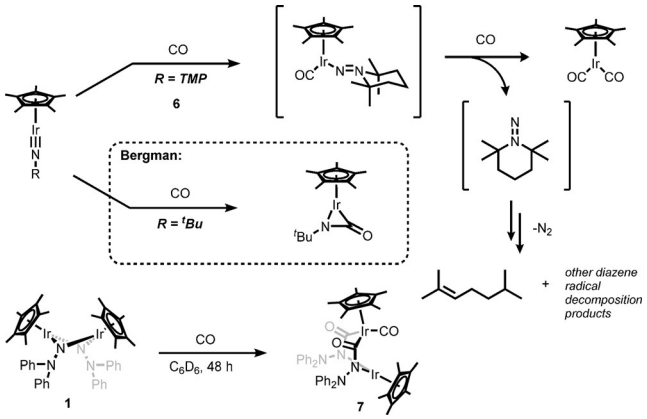

Scheme 2. Reactions of CO with Cp*IrNTMP (**6**) (top), Bergman's Cp*IrN^{t}Bu (middle), and [Cp*Ir(N_2Ph_2)]$_2$ (**1**) (bottom).

Exposure of a C_6D_6 solution of **6** to an atmosphere of CO yields a deep red solution, which over time results in the formation of Cp*Ir$(CO)_2$ and several organic byproducts, which were identified as decomposition products of free *N*-(2,2,6,6-tetramethylpiperidyl)nitrene.[33] In this case, we propose that coordination of CO leads to charge transfer from the hydrazido N_β lone pair to the Ir, formally reducing it from Ir^{III} to Ir^{I}. Then, the resulting 1,1-isodiazene can be displaced by CO, forming Cp*Ir$(CO)_2$ and the free nitrene, which decomposes in solution. In comparison, Cp*IrN*t*Bu and other related imido complexes react with CO to form η^2-bound organoisocyanates,[11] Thus, unlike normal terminal imidos, the nitrogen ligand of **6** undergoes CO-induced tautomerization rather than reacting directly with CO. Reactions of **6** with other L donors such as PMe_3 or outer-sphere oxidants such as $[Fc]^+[PF_6]^-$ also generate product mixtures from diazene decomposition, and traces of the analogous reduced product Cp*Ir$(PMe_3)_2$ were detectable by NMR. In contrast, the Ir–N bond in the dimeric hydrazidos behaves similarly to the bridging imidos of Group 9.[30] For example, **1** reacts with an atmosphere of CO to give the eventual generation of CO-inserted product **7**, which contains two inequivalent Ir centers. The crystal structure of **7** is shown in Figure 4.

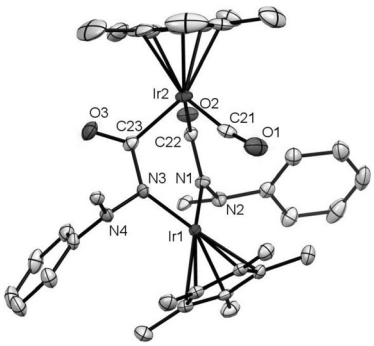

Figure 4. ORTEP of compound **7**.[35] Thermal ellipsoids are drawn at 50% probability. Hydrogen atoms have been omitted and two phenyl rings have been reduced to *ipso* carbons for clarity. Selected bond lengths [Å] and angles [°]: Ir1–N1 2.020(3), Ir1–N3 2.022(3), N1–N2 1.429(4), N3–N4 1.418(4), Ir2–C21 1.842(4), Ir2–C22 2.044(4), Ir2–C23 2.046(4), C21–O1 1.143(5), C22–O2 1.222(4), C23–O3 1.225(5); Ir2-C21-O1 170.3(4).

Reaction of terminal hydrazidos with electrophiles also yields differential and remarkable reactivity. In the case of **6**, one could envision an electrophile such as MeI reacting in one of three ways: 1) Direct reaction with the HOMO (predominantly N_β lone pair), 2) attack of the electrophile by the Ir metal center in an S_N2-like fashion, or 3) reaction across the Ir–N bond in analogy to Cp*IrN*t*Bu, which ultimately gives $[^t BuNMe_3]^+I^-$ and $[Cp^*IrI_2]_2$. Remarkably, the reaction of **6** with stoichiometric MeI produces complex **8**, the apparent product of a nucleophilic attack by an Ir^{III} center on MeI (Scheme 3). **8** is isolated as a mixture of diastereomers, both of which can be crystallized. Their solid-state structures are reported in Figure 5.

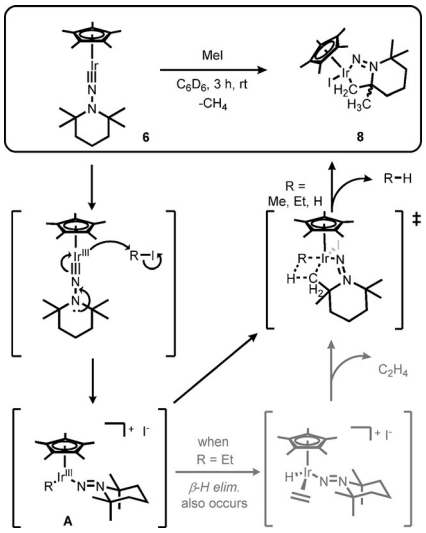

Scheme 3. Reaction of Cp*IrNTMP (**6**) with methyl iodide to produce compound **8** with the loss of methane. The proposed mechanism for the formation of **8** is also shown, showing the concerted nucleophilic attack and hydrazido(2−) oxidation to form intermediate **A**. When using ethyl iodide, competitive β-H elimination allows for the formation of ethylene as well as compound **8**.

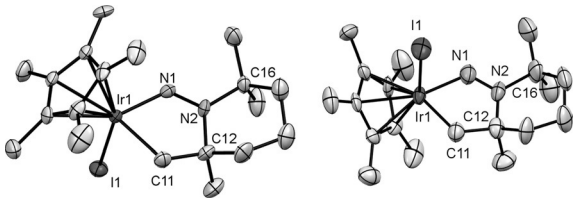

Figure 5. ORTEP of both diasteromers of compound **8**.[35] Thermal ellipsoids are drawn at 50% probability. Hydrogen atoms and one crystallographically independent molecule in **8b** have been omitted for clarity. Selected bond lengths [Å] and angles [°] for **8a**: Ir1–N1 1.936(6), N1–N2 1.249(8), Ir1–C11 2.107(7), Ir1–I1 2.6881(8); Ir1-N1-N2 121.5(5), C12-N2-C16 122.7(4).

The structure of **8** shows an elongated Ir–N bond distance of 1.939(6) Å as well as a shortened N_α–N_β distance of 1.249(8) Å, indicating double bond character between the nitrogens. Thus, the structural parameters of **8** demonstrate a formal oxidation of the hydrazido(2−) moiety to the neutral isodiazene ligand, similar to Hartwig's isolated isodiazene complex. This is the first instance of reagent-induced redox isomerism in a hydrazido(2−) moiety, in which the N_β lone pair ultimately provides an electron reservoir for reactivity at Ir.

The proposed mechanism for the formation of **8** is shown in Scheme 3. MeI undergoes a nucleophilic attack by Ir with concurrent electron transfer from the N_β to Ir. This redox non-innocent electron transfer from hydrazide(2−) to isodiazene helps to avoid the intermediacy of the Ir^V oxidation state. The resulting Ir^{III} methyl isodiazene structure **A** can then undergo σ-bond metathesis with a proximal piperidine methyl group to form the cyclometallated product **8**, with concomitant loss of methane. The reaction of **6** with CD_3I in C_6D_6 carried out in a sealed J-Young tube shows a peak for CD_3H, confirming the production of methane. At this stage, the exact nature of the tautomerization mechanism and its degree of concertedness remain ambiguous: the arrow-pushing designation in Scheme 3 is used simply to indicate that tautomerization occurs while the complex is undergoing reaction.

Complex **8** can also be formed from the reaction of **6** with ethyl iodide. The kinetics of the reaction are slower, as would be expected for an S_N2-type nucleophilic attack by Ir.[34] In addition to the expected ethane byproduct, ethylene is also observed in the reaction mixture by using ^1H NMR spectroscopy. The generation of ethylene presumably occurs through a competitive β-H elimination from the ethyl intermediate **A** followed by an intramolecular σ-bond metathesis of the resulting iridium hydride with the piperidine methyl group.

In summary, monomeric iridium terminal hydrazido(2−) complexes can be synthesized using bulky, alkyl 1,1-organohydrazines. Cp*IrNTMP displays a short, linear Ir–N linkage indicative of triple bonding. The Ir–N_α–N_β moiety displays remarkable redox non-innocent behavior in all characterized cases; reactions with neutral CO result in the formally reduced $Cp^*Ir(CO)_2$, while reactions with electrophiles result in a net oxidation of the ligand rather than the metal center. We are currently exploring redox catalytic applications of this new moiety on Ir and related late transition metal centers.

Acknowledgements

Financial support was provided by the University of Minnesota (start-up funds) and the ACS Petroleum Research Fund (ACS-PRF 54225-DNI3). The Bruker-AXS D8 Venture diffractometer was purchased through a grant from NSF/MRI (1224900) and the University of Minnesota. Equipment purchases for the NMR facility were supported through a grant from the NIH (S10OD011952) with matching funds from the University of Minnesota. The Minnesota Supercomputing Institute (MSI) at the University of Minnesota provided resources that contributed to the results reported within this paper. We would like to thank Kari Kusler for assistance with DFT calculations, as well as Dr. Victor Young for help with crystal structure solutions.

Keywords: hydrazide ligands · iridium complexes · organometallic chemistry · redox non-innocence · triple bonds

How to cite: *Angew. Chem. Int. Ed.* **2016**, *55*, 13169–13173
Angew. Chem. **2016**, *128*, 13363–13367

[1] S. T. Kleespies, W. N. Oloo, A. Mukherjee, L. Que, *Inorg. Chem.* **2015**, *54*, 5053–5064.
[2] V. Lyaskovskyy, A. I. O. Suarez, H. Lu, H. Jiang, X. P. Zhang, B. de Bruin, *J. Am. Chem. Soc.* **2011**, *133*, 12264–12273.
[3] R. H. Perry, T. J. Cahill, J. L. Roizen, J. Du Bois, R. N. Zare, *Proc. Natl. Acad. Sci. USA* **2012**, *109*, 18295–18299.
[4] G.-Y. Gao, J. E. Jones, R. Vyas, J. D. Harden, X. P. Zhang, *J. Org. Chem.* **2006**, *71*, 6655–6658.
[5] X. Dai, P. Kapoor, T. H. Warren, *J. Am. Chem. Soc.* **2004**, *126*, 4798–4799.
[6] D. M. Jenkins, T. A. Betley, J. C. Peters, *J. Am. Chem. Soc.* **2002**, *124*, 11238–11239.
[7] R. E. Cowley, R. P. Bontchev, J. Sorrell, O. Sarracino, Y. Feng, H. Wang, J. M. Smith, *J. Am. Chem. Soc.* **2007**, *129*, 2424–2425.
[8] L. Zhang, Y. Liu, L. Deng, *J. Am. Chem. Soc.* **2014**, *136*, 15525–15528.
[9] J. Du, L. Wang, M. Xie, L. Deng, *Angew. Chem. Int. Ed.* **2015**, *54*, 12640–12644; *Angew. Chem.* **2015**, *127*, 12831–12835.
[10] D. J. Mindiola, G. L. Hillhouse, *J. Am. Chem. Soc.* **2001**, *123*, 4623–4624.
[11] A. M. Geer, C. Tejel, J. A. López, M. A. Ciriano, *Angew. Chem. Int. Ed.* **2014**, *53*, 5614–5618; *Angew. Chem.* **2014**, *126*, 5720–5724.
[12] R. E. Cowley, P. L. Holland, *Inorg. Chem.* **2012**, *51*, 8352–8361.
[13] J. S. Anderson, G. E. Cutsail, J. Rittle, B. A. Connor, W. A. Gunderson, L. Zhang, B. M. Hoffman, J. C. Peters, *J. Am. Chem. Soc.* **2015**, *137*, 7803–7809.
[14] A. D. Schofield, A. Nova, J. D. Selby, C. D. Manley, A. D. Schwarz, E. Clot, P. Mountford, *J. Am. Chem. Soc.* **2010**, *132*, 10484–10497.
[15] T. Gehrmann, J. Lloret Fillol, S. A. Scholl, H. Wadepohl, L. H. Gade, *Angew. Chem. Int. Ed.* **2011**, *50*, 5757–5761; *Angew. Chem.* **2011**, *123*, 5876–5881.
[16] H. Herrmann, J. Lloret Fillol, H. Wadepohl, L. H. Gade, *Angew. Chem. Int. Ed.* **2007**, *46*, 8426–8430; *Angew. Chem.* **2007**, *119*, 8578–8582.
[17] V. Lyaskovskyy, B. de Bruin, *ACS Catal.* **2012**, *2*, 270–279.
[18] I. A. Tonks, A. C. Durrell, H. B. Gray, J. E. Bercaw, *J. Am. Chem. Soc.* **2012**, *134*, 7301–7304.
[19] A. J. Clulow, J. D. Selby, M. G. Cushion, A. D. Schwarz, P. Mountford, *Inorg. Chem.* **2008**, *47*, 12049–12062.
[20] I. A. Tonks, J. E. Bercaw, *Inorg. Chem.* **2010**, *49*, 4648–4656.

[21] S. Banerjee, A. L. Odom, *Dalton Trans.* **2008**, 2005 – 2008.
[22] S. Patel, Y. Li, A. L. Odom, *Inorg. Chem.* **2007**, *46*, 6373 – 6381.
[23] Y. Li, Y. Shi, A. L. Odom, *J. Am. Chem. Soc.* **2004**, *126*, 1794 – 1803.
[24] A. A. Danopoulos, G. Wilkinson, D. J. Williams, *J. Chem. Soc. Dalton Trans.* **1994**, 907.
[25] C. Bustos, C. Manzur, D. Carrillo, F. Robert, P. Gouzerh, *Inorg. Chem.* **1994**, *33*, 1427 – 1433.
[26] D. V. Yandulov, R. R. Schrock, *J. Am. Chem. Soc.* **2002**, *124*, 6252 – 6253.
[27] R. B. Siedschlag, V. Bernales, K. D. Vogiatzis, N. Planas, L. J. Clouston, E. Bill, L. Gagliardi, C. C. Lu, *J. Am. Chem. Soc.* **2015**, *137*, 4638 – 4641.
[28] Z. Huang, J. S. Zhou, J. F. Hartwig, *J. Am. Chem. Soc.* **2010**, *132*, 11458 – 11460.
[29] D. S. Glueck, J. Wu, F. J. Hollander, R. G. Bergman, *J. Am. Chem. Soc.* **1991**, *113*, 2041 – 2054.
[30] C. Tejel, M. A. Ciriano, S. Jiménez, V. Passarelli, J. A. López, *Inorg. Chem.* **2008**, *47*, 10220 – 10222.
[31] D. Dobbs, R. G. Bergman, *Organometallics* **1994**, *13*, 4594 – 4605.
[32] G. Parkin, A. Van Asselt, D. J. Leahy, L. Whinnery, N. G. Hua, R. W. Quan, L. M. Henling, W. P. Schaefer, B. D. Santarsiero, J. E. Bercaw, *Inorg. Chem.* **1992**, *31*, 82 – 85.
[33] W. D. Hinsberg, P. G. Schultz, P. B. Dervan, *J. Am. Chem. Soc.* **1982**, *104*, 766 – 773.
[34] J. A. Labinger, *Organometallics* **2015**, *34*, 4784 – 4795.
[35] CCDC 1497530 (**1**), 1497529 (**2**), 1497531 (**4**), 1497536 (**6**), 1497532 (**7**), 1497534 (**8a**), and 1497535 (**8b**) contain the supplementary crystallographic data for this paper. These data are provided free of charge by The Cambridge Crystallographic Data Centre.

Received: August 6, 2016
Published online: September 21, 2016

